Influence of misfit dislocations on the magnetoresistance of MgO-based epitaxial magnetic tunnel junctions

F. Bonell, S. Andrieu,* C. Tiusan, and F. Montaigne
Institut Jean Lamour, Nancy Université/CNRS, BP 239, 54506 Vandœuvre-lès-Nancy, France

E. Snoeck, B. Belhadji, and L. Calmels
CEMES, Université de Toulouse/CNRS, BP 94347, F-31055 Toulouse Cedex 4, France

F. Bertran, P. Le Fèvre, and A. Taleb-Ibrahimi
SOLEIL Synchrotron, CNRS–UR1, Saint-Aubin, 91192 Gif-sur-Yvette Cedex, France
(Received 4 June 2010; revised manuscript received 2 September 2010; published 29 September 2010)

Magnetotransport in epitaxial magnetic tunnel junctions is investigated while varying the density of dislocations in the MgO barrier. Fe-V alloys with variable composition and lattice mismatch with MgO are used as electrodes. The reduction in the dislocation density was probed by reflection high-energy electron diffraction and high-resolution electron microscopy. Spin-resolved photoemission together with first-principles calculations were used to study the Δ bands in the alloys. Although their polarization decreases upon alloying, the tunnel magnetoresistance is enhanced for low V content as a consequence of the better structural coherency. Our results demonstrate the direct relation between the density of dislocations in the epitaxial barrier and the tunnel magnetoresistance amplitude.

DOI: 10.1103/PhysRevB.82.092405 PACS number(s): 75.70.Cn, 72.25.Mk, 73.40.Gk, 73.40.Rw

In the framework of coherent tunneling, a tunnel magnetoresistance (TMR) well above 1000% is expected for Fe/MgO/Fe(001) magnetic tunnel junctions (MTJs) as a result of the full polarization of Δ_1 Bloch states in Fe and of the symmetry filtering in MgO.[1] Indeed, fully epitaxial Fe/MgO/Fe(001) MTJs grown by molecular beam epitaxy (MBE) exhibit a large TMR but it is limited to 250% at low temperature.[2] The large ratios reached with Fe-Co alloys[3] and bcc Co (Ref. 4) lie also well below theoretical expectations.[5] Understanding the origin of this apparent limitation is a fundamental issue to accurately control spin-polarized tunneling. This has motivated many theoretical studies but experimental investigations remain scarce. Here, we address this question and focus on the model Fe/MgO/Fe(001) stack. The intrinsic oxidation of Fe at the Fe/MgO interface could possibly explain the large deviation from theoretical expectations.[6,7] Nevertheless, we have recently shown that in real MTJs, oxygen doping of the interface has a weak effect on the TMR amplitude.[8] Theoretically, oxygen vacancies in the MgO barrier should also decrease the TMR.[9] However, their presence has not been evidenced unambiguously. Other defects definitely exist in the barrier. Dislocations due to the rather large misfit between Fe and MgO (3.9%) (Refs. 2 and 10–13) were clearly evidenced by high-resolution transmission electron microscopy (HRTEM) (Ref. 2) but their effect on tunneling is not yet established, neither by calculations nor experimentally. In this Brief Report, we demonstrate the strong influence of misfit dislocations and show that reducing their density strongly enhances the TMR.

In this goal, we propose to replace the Fe electrodes by a ferromagnetic alloy having a lattice parameter closer to that of MgO. This alloy must exhibit an energy diagram similar to that of bcc Fe, to preserve the specificities of the electrode band structure, with fully polarized Δ_1 states for large TMR values. For this purpose we chose to replace Fe by Fe-V alloys because of the large lattice parameter of V (0.303 nm to compare with 0.287 nm for Fe and 0.298 nm for MgO[110]) and because of the well-defined bcc structure of these alloys. We show by electron diffraction [reflection high-energy electron diffraction (RHEED)] and HRTEM experiments that the crystalline quality of the MgO barrier grown on these alloys is actually improved. Spin-resolved ultraviolet photoelectron spectroscopy (SR-UPS) measurements combined with symmetry-resolved density of states calculations were used to investigate the spin polarization of the Δ states at the Fe-V/MgO interface, a crucial parameter for TMR. Finally, the magnetotransport in MTJs is analyzed taking into account the polarization of the electrodes and the dislocation density in the barrier.

The multilayers were grown by MBE on MgO(001) substrates. The growth and microfabrication details are similar to those given in Ref. 8. Fe and V were coevaporated at rates around 1 nm/min. The stoichiometry of the Fe-V alloys was fixed by adjusting the Fe and V fluxes measured by a quartz microbalance, and checked by x-ray photoemission spectroscopy measuring the Fe $2p$ and V $2p$ core levels. The thickness of the MgO barrier was fixed to 12 monolayers (MLs), which gives a TMR of 180% at room temperature (RT) with Fe electrodes. This thickness was accurately controlled during the growth by measuring the RHEED intensity oscillations.

A perfect matching between Fe-V and MgO lattices is reached for 70% of V.[10] However, since the films are not ferromagnetic at RT for more than 50% of V,[10] we limited our study to V concentrations ranging from 0% to 30%. Consequently, the plastic relaxation of MgO takes place at a finite critical thickness h_c. Note that the smaller the misfit is, the higher h_c and the smaller the dislocation density are. h_c was determined using RHEED, by measuring the variations in the average surface lattice parameter during the growth of

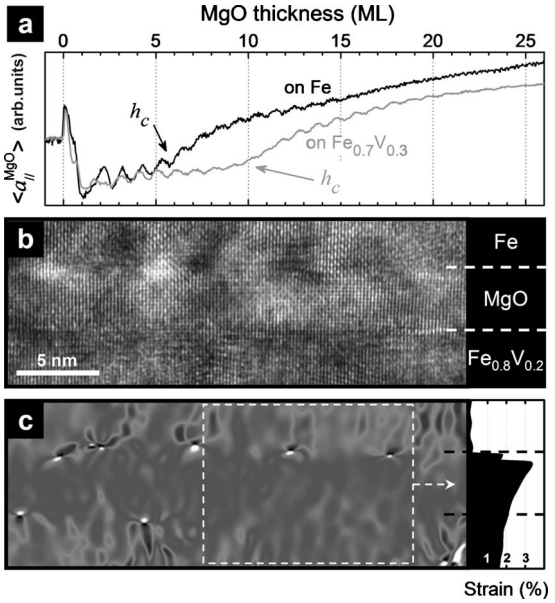

FIG. 1. (a) Variation in the average surface in-plane lattice spacing of MgO measured by RHEED during the growth on Fe(001) and on $Fe_{0.7}V_{0.3}$(001). The critical thickness of plastic relaxation h_c is indicated. (b) HR-TEM image of a single-crystal $Fe_{0.8}V_{0.2}$/MgO(2.7 nm)/Fe(001) MTJ in the Fe[110] zone axis. (c) Map of strain in atomic planes normal to the interface [(200)MgO and (110)Fe]. Dislocation cores appear as highly contrasted spots. Their density is higher at the MgO/Fe interface than at the Fe-V/MgO one. The graph shows a profile of strain across the barrier, integrated in the zone delimited by the white borders.

MgO on Fe-V(001). During the pseudomorphic growth, this lattice parameter is equal to that of the buffer layer. When the plastic relaxation sets in, the strain is partially relaxed in the vicinity of the cores of nucleating dislocations and the average surface lattice parameter suddenly increases [Fig. 1(a)]. h_c substantially increases with the V content. It reaches 5–6 ML for an Fe(001) supporting layer and 9–10 ML with $Fe_{0.7}V_{0.3}$(001) [Figs. 1(a) and 1(b)]. These values are consistent with those expected for the appearance of $\frac{1}{2}\langle 011\rangle\{011\}$ dislocations (Fig. 2). In this case, following Vassent *et al.*, h_c is given by the formula:[11]

$$h_c = \frac{b}{4\sqrt{2}\pi(1+\nu)}\left|1+\frac{1}{f}\right|\ln\left(\frac{\alpha h_c}{b}\right),$$

where the modulus of the Burger vector is $b=a_{MgO}/\sqrt{2}$, the Poisson ratio $\nu=0.173$ (from Ref. 11), the misfit $f=(a_{MgO}-a_{Fe\text{-}V}\sqrt{2})/a_{Fe\text{-}V}\sqrt{2}$ and α is a parameter linked to the core radius and core energy of a dislocation. The average in-plane lattice parameter $a_{Fe\text{-}V}$ was directly measured by x-ray diffraction.[10] The values of h_c obtained using this formula as a function of the misfit f are plotted in Fig. 2 for α between 3.1 and 4.3. The agreement with the experiments—on different Fe-V alloys, for different V concentrations, including pure Fe—is very good. This shows that, apart from the increasing critical thickness, the plastic relaxation mechanisms are similar during the growth on Fe and on Fe-V alloys.

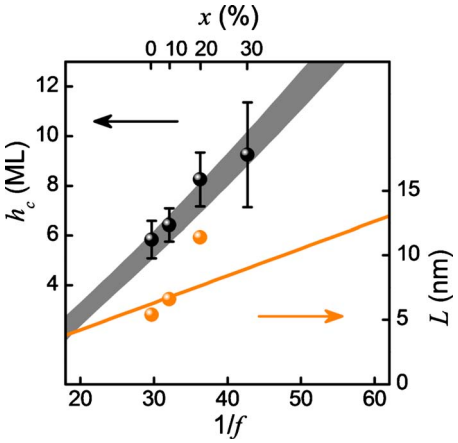

FIG. 2. (Color online) Left axis—MgO critical thickness of plastic relaxation on $Fe_{1-x}V_x$(001) measured by RHEED versus the misfit f and vanadium content x of the alloy. The gray strip is the calculated range of critical thicknesses (see text). Right axis—average distance between dislocations at the $Fe_{1-x}V_x$/MgO bottom interface in MgO/$Fe_{1-x}V_x$/MgO/Fe/Co/Au MTJs, measured by HRTEM. The line gives the $a_{MgO}/2f$ value expected if the dislocations totally relieve the misfit strain.

An HRTEM image of an $Fe_{0.8}V_{0.2}$(50 nm)/MgO(12 ML)/Fe(20 nm)/Co/Au MTJ is shown in Fig. 1(b). Figure 1(c) shows the corresponding strain map calculated with the procedure given in Ref. 14. The dislocation cores, where the strain is large, appear as highly contrasted spots. Strain then goes down to zero between two dislocations. Obviously, the dislocation density is much smaller at the Fe-V/MgO interface than at the MgO/Fe one. The average distance L between adjacent dislocations was measured by counting the cores at Fe-V/MgO interface over 250 nm for each sample. L is equal to 5.2 nm at the Fe/MgO interface and reaches 11.2 nm at the $Fe_{0.8}V_{0.2}$/MgO one (see Fig. 2). Therefore, moderate V concentrations are sufficient to decrease the dislocation density by more than a factor of 2. It should be noted that the dislocation density in such complete stackings is much larger than the one previously reported for *free* MgO films deposited on Fe(001).[13] This difference is obviously due to the presence of a top layer. This layer induces additional strain on the barrier which may favor the propagation of the dislocations. As a result, L is found to be close to the value $a_{MgO}/2f$ expected from a crude static model, in which the lattice parameter in each layer is equal to the bulk value. In this case, the dislocations totally relieve the misfit strain (Fig. 2). However, for more than 10% of V in the bottom layer, the model does not fit to the data since $L > a_{MgO}/2f$, which means that the 12 ML MgO film remains partially strained.

Used as the supporting bottom electrode, the Fe-V alloys make a clear improvement of the barrier crystallinity. On the other hand, the magnetoresistance is highly dependent on the magnetic/electronic properties of the electrodes, and, in particular, on the spin polarization of the Δ bands.[1,5] In order to measure it, we have performed SR-UPS experiments on the CASSIOPEE beamline of the SOLEIL synchrotron light source on Fe-V(50 nm)/MgO(2 ML) samples. The spectra were recorded at RT using 60 eV photons. The beam was

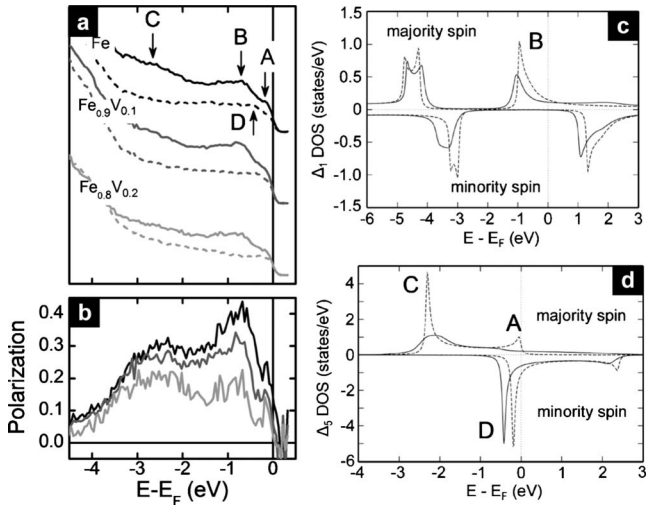

FIG. 3. Left—(a) SR-UPS spectra measured on Fe-V(001)/MgO(2 ML) at $\bar{\Gamma}$ for majority spins (solid line) and minority spins (dashed line) and (b) corresponding spin polarization. Right—spin resolved and relativistic (SPR)-KKR calculated density of states for majority and minority spins for pure Fe (dashed line) and $Fe_{0.8}V_{0.2}$ (full line) for (c) Δ_1 symmetry and (d) Δ_5 symmetry.

p-polarized and the incident angle was set to 45°. The photoelectron detection was performed along the [001] normal axis of the films which corresponds to the Δ direction in the reciprocal space. Thanks to the small angular acceptance of the detector ($\pm 1.8°$), only $\pm 6\%$ of the first surface Brillouin zone around the $\bar{\Gamma}$ point was probed, the resolution in k being $\Delta k_{\parallel} = \pm 0.13$ Å^{-1}. The overall energy resolution was set to 170 meV. In this geometry, dipolar selection rules ensure that the spin-resolved spectra only reflect the polarization of Δ_1 and Δ_5 states.[15] Figure 3(a) shows the majority ($N_\uparrow$) and minority ($N_\downarrow$) photoemission spectra obtained on Fe/MgO, $Fe_{0.9}V_{0.1}$/MgO, and $Fe_{0.8}V_{0.2}$/MgO. The corresponding spin polarizations P, given by $P=(N_\uparrow - N_\downarrow)/(N_\uparrow + N_\downarrow)$, are plotted in Fig. 3(b). All spectra exhibit a large increase in intensity below −3.5 eV binding energy (BE) for both majority and minority spins, which results in a drop of the polarization. This nonpolarized signal originates from the valence states of the top MgO layer. Between 0 and −3 eV BE, in the MgO band gap, the metal-layer electronic states appear. For Fe/MgO as well as Fe-V/MgO, majority-spin spectra show three emission peaks, at −0.2 eV (peak A), −0.7 eV (peak B), and −2.5 eV (peak C) BEs. The minority-spin spectra exhibit only one peak at −0.5 eV BE (peak D). Emission peaks are usually indexed in terms of direct interband transitions between a certain Δ_1 or Δ_5 initial state and a final freelike Δ_1 state. For an excitation energy of 60 eV, the escape depth of photoelectrons is almost minimal and on the order of a few angstrom. Therefore, the quantum uncertainty on the photoelectron wave vector is a non-negligible fraction of the Brillouin zone. In this case, the emission spectra more reflects the spin-resolved density of Δ_1 and Δ_5 states at energy E (convoluted with the quasiconstant Δ_1 DOS at energy $E+60$ eV).[16] The electronic structure of Fe-V alloys at 0 K has been calculated using the Korringa Kohn Rostoker (KKR) Green's-function method based on the density-functional theory, together with the coherent-potential approximation to account for chemical disorder.[17] The one-dimensional Δ_1 and Δ_5 partial DOS have been obtained using the Bloch spectral function $A(\mathbf{k};E)$. The calculations were performed for different V concentrations. The Δ_1 and Δ_5 DOS calculated for Fe and an $Fe_{0.8}V_{0.2}$ random alloy are shown in Fig. 3. The peaks indexed by the letters A–D in the spin-resolved DOS curves correspond to band extrema and their energy position are in excellent agreement with the measured A–D peaks. The peaks below −3 eV BE are masked by MgO valence states in the experimental photoemission spectra. Furthermore, the intensities of the different experimental peaks in majority-spin spectra (A, B, and C) are smoothed when V is incorporated. The calculations account for this behavior, which is due to the substitutional disorder in the alloy. In minority-spin spectra, the peaks are believed to be smoothed out by the MgO capping layer[15] but this behavior remains unclear. These results demonstrate that the V doping of bcc Fe does not strongly affect the specific pure Fe *occupied* DOS, at least in the V concentration range studied here. This is also supported by the conductance curves measured on MTJs in the range −1 to 1 V which are very similar to those obtained on Fe/MgO/Fe. Importantly, the polarization of Δ_1 states remains equal to 100% in Fe-V alloys. Consequently, Fe-V/MgO/Fe-V MTJs should provide a large TMR. On the other hand, the global polarization of Δ states gradually decreases when the V concentration increases, in particular, at the Fermi energy [Fig. 3(b)]. Such a decrease is detrimental for the TMR but it will be useful in the following to disentangle the respective influence of dislocations and polarization on the TMR.

To quantify independently the effects of the structural quality of the barrier and of the spin polarization on the TMR, we patterned two series of MTJs. It should be noted that the typical resistances of a 10×10 μm^2 MTJs are around 1 MΩ, which clearly eliminate the possibility of having pinholes in the barrier. The first series is made of a bottom Fe electrode, an MgO barrier (where the dislocation density is high because of the large lattice mismatch) and a top Fe-V electrode (with a lower spin polarization than the bottom Fe electrode). A decrease in the TMR with V concentration is thus expected compared to the Fe/MgO/Fe reference MTJ. This is what we actually observed, as shown in Fig. 4. In the second series, the MgO barrier is grown on an Fe-V bottom electrode, which leads to improvement of the crystalline quality of the barrier. To compare with the first series of MTJs, we used Fe as the top electrode, in order to get the same couple of polarizations for the top and bottom electrodes. In that case, the TMR is found to increase up to 240% at RT for about 10% of V. Then, it slowly decreases for larger V concentrations. The TMR remains larger than in the Fe/MgO/Fe MTJs, up to 20% of V in the bottom electrode. These results can be easily understood. At low V concentration, the spin polarization is not yet significantly decreased but the better crystalline quality of the MgO barrier improves the TMR. When V concentration is increased, there is a competition between the improvement of the barrier quality and the decrease in the spin polarization in the Fe-V electrode. To definitely support this conclusion, we also prepared MTJs with two similar $Fe_{1-x}V_x$ electrodes. For $x=0.1$,

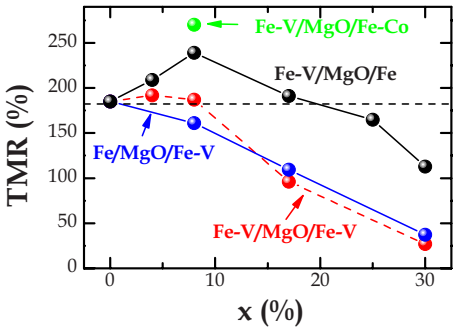

FIG. 4. (Color online) TMR variation at RT versus V concentration x for the different series of MTJs (see text). The dashed line at 180% corresponds to Fe/MgO/Fe TMR value.

the TMR is in between the TMR obtained for the two former series. However, for $x>0.1$, the drop in the TMR is more pronounced, as expected since the polarization of *both* electrodes decreases. Finally, we used a $Fe_{0.9}V_{0.1}$ as the bottom electrode and a top electrode made of bcc Fe-Co alloy, in which *all* the Δ states are fully polarized at the Fermi energy.[5] Different alloy compositions were tested up to 50% of Co. The largest TMR reaches 270% at RT and was obtained with $Fe_{0.75}Co_{0.25}$ (Fig. 4). This value is larger than the largest TMR of FeV/MgO/Fe MTJs, supporting our conclusions on the influence of the spin polarization in the electrodes.

The large improvement of TMR obtained by reducing the dislocations density may be surprising since the latter appear as punctual defects at interfaces in HRTEM images. However, we emphasize that dislocations are in fact extended defects. $\frac{1}{2}\langle 011\rangle\{011\}$ dislocations are created by glide of the {001} planes which are oriented at 45° from the interfaces.[11,12] As a consequence, the barrier is strained over the entire glide zone, that is to say, over a distance t along the interface for an MgO thickness t. Knowing the average distance between dislocations $L=5.2$ nm at the Fe/MgO interface, an important fraction $t/L=50\%$ of the barrier is strained in a typical Fe/MgO($t=2.6$ nm)/Fe MTJ. It was shown that this strain results in a tilting of several degrees of the MgO(001) planes.[12] In these tilted segments, the Δ direction within the barrier does not match anymore the Δ direction in the electrodes. This means that dislocations break the in-plane crystalline periodicity at the interfaces, which in turn alters the symmetry filtering by MgO.

In summary, we showed that misfit dislocations in the MgO barrier strongly influence the TMR in MTJs. Despite the decrease in the Δ spin polarization in Fe-V alloys, the decrease in the dislocation density due to the smaller misfit with MgO enhances the TMR up to 240% at RT for $Fe_{0.9}V_{0.1}$/MgO/Fe(001) MTJs. Improving the crystalline quality of the barrier may also be an efficient way of reducing the electric noise level and increasing the breakdown voltage. Finally, we suggest that our results may also explain why larger TMR is measured with sputtered FeCoB/MgO-based MTJs. In this case, the MgO barrier is grown on amorphous FeCoB. The mechanisms of plastic relaxation and the dislocations density are therefore very different. Understanding the appearance of such defects during growth/crystallization may thus be one of the key points to reach even higher TMR values.

We acknowledge support from the ANR under Contract No. BLAN07-188976 (SPINCHAT). The calculations presented in this Brief Report have been performed at the CALMIP/UPS Toulouse parallel computer center. The HRTEM analysis is supported by the French CNRS and CEA "METSA" network.

*Corresponding author; stephane.andrieu@ijl.nancy-universite.fr

[1] W. H. Butler, X.-G. Zhang, T. C. Schulthess, and J. M. MacLaren, Phys. Rev. B **63**, 054416 (2001).
[2] S. Yuasa *et al.*, Nature Mater. **3**, 868 (2004); C. Tiusan *et al.*, J. Phys.: Condens. Matter **19**, 165201 (2007).
[3] S. Ikeda *et al.*, Appl. Phys. Lett. **93**, 082508 (2008).
[4] S. Yuasa *et al.*, Appl. Phys. Lett. **87**, 222508 (2005).
[5] X.-G. Zhang and W. H. Butler, Phys. Rev. B **70**, 172407 (2004).
[6] X. G. Zhang, W. H. Butler, and A. Bandyopadhyay, Phys. Rev. B **68**, 092402 (2003).
[7] H. L. Meyerheim *et al.*, Phys. Rev. Lett. **87**, 076102 (2001).
[8] F. Bonell *et al.*, Phys. Rev. B **79**, 224405 (2009).
[9] J. P. Velev *et al.*, Appl. Phys. Lett. **90**, 072502 (2007).
[10] F. Bonell *et al.*, IEEE Trans. Magn. **45**, 3467 (2009); D. Herranz *et al.*, Appl. Phys. Lett. **96**, 202501 (2010).
[11] J.-L. Vassent *et al.*, J. Appl. Phys. **80**, 5727 (1996).
[12] M. Dynna, J. L. Vassent, A. Marty, and B. Gilles, J. Appl. Phys. **80**, 2650 (1996).
[13] M. Klaua *et al.*, Phys. Rev. B **64**, 134411 (2001).
[14] M. J. Hÿtch, E. Snoeck, and R. Kilaas, Ultramicroscopy **74**, 131 (1998).
[15] L.-N. Tong *et al.*, Phys. Rev. B **77**, 064421 (2008).
[16] P. J. Feibelman and D. E. Eastman, Phys. Rev. B **10**, 4932 (1974).
[17] H. Ebert *et al.*, SPR-KKR package v3.6, Munich, http://olymp.cup.uni-muenchen.de/ak/ebert/SPRKKR